Performance of a solar chimney by varying design parameters

Tichaona Kumirai, Researcher, Built Environment CSIR
Jan-Hendrik Grobler, DPSS CSIR
Dr D.C.U. Conradie, Senior researcher, Built Environment CSIR

1 Introduction

Trombe walls and solar chimneys are not widely used or well known in South Africa. A previous Green Building Handbook article described the University of Fort Hare teaching complex in East London (Stratford, 2012) that inter alia used a trombe system for a naturally ventilated building. This article explores the use of these passive devices further.

Solar chimneys are passive elements that use solar energy to induce a buoyancy force that drives airflow and naturally ventilate the building. Buoyancy refers to one of the mechanisms by which motion in fluids such as air is caused by natural means. Buoyancy forces are induced by density differences due to the variation of temperature of the fluid: warmer and thus lighter fluid rises and cooler and thus denser fluid sinks.

According to CIBSE (1997) the general formula that determines the flow rate through a solar chimney is:

$$Q = CA\sqrt{2gh\frac{T_i - T_o}{T_i}} \quad (1)$$

Q = stack effect draft/ draught flow rate (m³/s)

A = flow area (m²)

C = discharge coefficient (usually taken to be from 0.65 to 0.70)

g = gravitational acceleration (9.81 m/s²)

h = height or distance (m)

T_i = average inside temperature (K)

T_o = outside air temperature (K)

Figure 1: Equation (1) Stack effect in a building (CIBSE, 1997)

This indicates the following important aspects. The following factors that determine the flow rate (Q) is available and can be varied by the designer:

- Flow area (A) in m²
- Height or distance (h) of the solar chimney
- Average inside temperature (T_i) expressed in K.

The mechanism by which solar chimney naturally ventilates the building is illustrated in Figure 2. Solar radiation enters the chimney through the glazed part and heats up the walls.

The temperature of the air inside the solar chimney channel rises due to heat transfer from the walls. If the temperature difference between the air in the solar chimney channel and the building is high enough, then the buoyancy forces drives the air from the interior of the building into the solar chimney channel to be exhausted at its top. The exhaust air is replaced by fresh air through openings or alternative paths in the building, and natural ventilation is accomplished.

Unlike mechanical ventilation where airflow is noticeable, since a fan is used to transfer momentum to the air to move in a certain direction, the airflow driven by solar chimney is often not noticeable because of the small pressure differences that lead to low velocities (Cengel, 2002). Because of the small buoyancy forces developed in a solar chimney, it is very important to optimise the design of solar chimneys to ensure optimal performance. The purpose of this chapter is to discuss the performance of an example solar chimney by varying the design parameters and examining their effects on the interior ventilation performance.

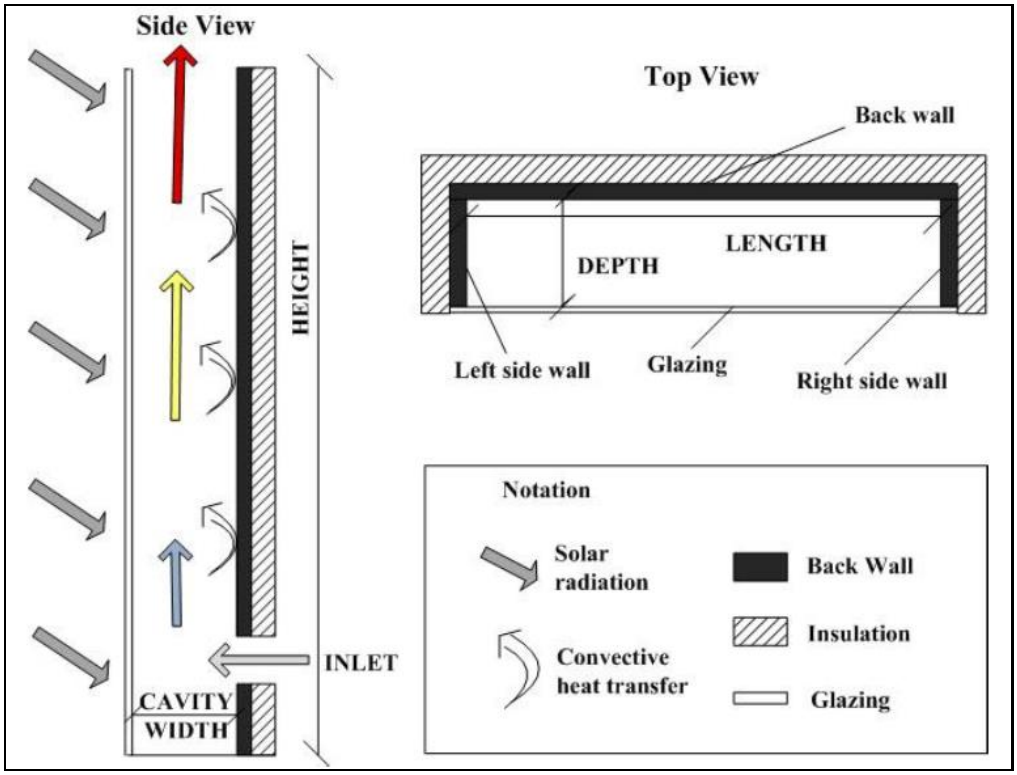

Figure 2: Illustration of solar chimney (Gontikaki, 2010, p.3).

1.1 Analysis objectives

i. The effect of chimney wall temperature on interior ventilation performance.
ii. The effect of floor grille width on the interior ventilation performance.
iii. The effect of chimney height on the interior ventilation performance.
iv. The effect of chimney inlet position on the interior ventilation performance.
v. The effect of chimney inlet area on the interior ventilation performance.

1.2 Description of bio-composite building

The solar chimney described in this chapter forms part of an experimental building the CSIR is undertaking to test the feasibility of constructing a net zero building, i.e. energy, water, waste, emissions, and biodiversity loss. To achieve this outcome significant emphasis is

placed on passive design principles, hence the use of a solar chimney to assist in ventilation and cooling.

2 Methodology

To quantify the effect of the abovementioned objectives, a numerical simulation (mathematical modelling) methodology was used. The simulations shown here were all performed with the commercial Computational Fluid Dynamics (CFD) code Star-CCM+. Star-CCM+ that utilises the finite volume method in its computations.

2.1 Brief description of the CFD finite volume method

The Navier-Stokes equations (NSE) are used to describe the motion of fluids. The NSE is based on the principle of the conservation of momentum, but the continuity equation (based on the conservation of mass) and the energy equation (based on the conservation of energy) are usually included. The conservation of mass, momentum and energy are given below by equations (2), (3) and (4), respectively. The formulations use index notation, where $i \in \{1, 2, 3\}$; $j \in \{1, 2, 3\}$.

$$\frac{\partial \rho}{\partial t} + \frac{\partial}{\partial x_j}\left[\rho u_j\right] = 0 \tag{2}$$

$$\frac{\partial}{\partial t}(\rho u_i) + \frac{\partial}{\partial x_j}\left[\rho u_i u_j + p\delta_{ij} - \tau_{ij}\right] = 0 \tag{3}$$

$$\frac{\partial}{\partial t}(\rho e_0) + \frac{\partial}{\partial x_j}\left[\rho u_j e_0 + u_j p + q_j - u_i \tau_{ij}\right] = 0 \tag{4}$$

These equations can be solved analytically in some cases, but have no known general analytical solution. The finite volume method is frequently used to transform the NSE from their partial differential form to algebraic equations, which can be solved numerically with the aid of a computer.

The term “finite volume” refers to non-overlapping volumes surrounding a number of discrete node points where values are calculated. The divergence theorem is used to convert the volume integrals to surface integrals. For example, if the divergence theorem is applied to equation (2), it takes the following form:

$$\frac{\partial}{\partial t}\int_V (\rho u_i) dV + \oint_A \left(\rho u_i u_j\right) n_j dA + \oint_A p\delta_{ij} n_j dA - \oint_A \tau_{ji} n_j dA = 0 \tag{5}$$

Once in this form, a set of algebraic equations can be obtained that describe how the flow variables change in each volume as a function of time. A detailed discussion of this process is not included here because a large number of methods have been developed to make adaptions to this basic technique for specific purposes. These include different methods to approximate flow properties at the faces; performing Reynolds-averaging to enable the introduction of turbulence modelling; and modifications to allow the modelling of inter alia multiphase flow.

2.2 CFD Solver settings

Figure 3 is an illustration of the bio-composite building. The two solar chimneys can be clearly seen.

Figure 3: An artist's impression of the completed bio-composite building.

For simulation purposes the flow was assumed to have reached a steady state and approximately 650 000 volumes (Figure 4) also referred to as cells were used in each model. The air was assumed to behave as an ideal gas. Turbulence was modelled using the CFD k-ε turbulence model. Since the flow is driven by buoyancy effects, density gradients were important and therefore the “coupled solver”-option was selected as opposed to the standard “segregated solver”-option.

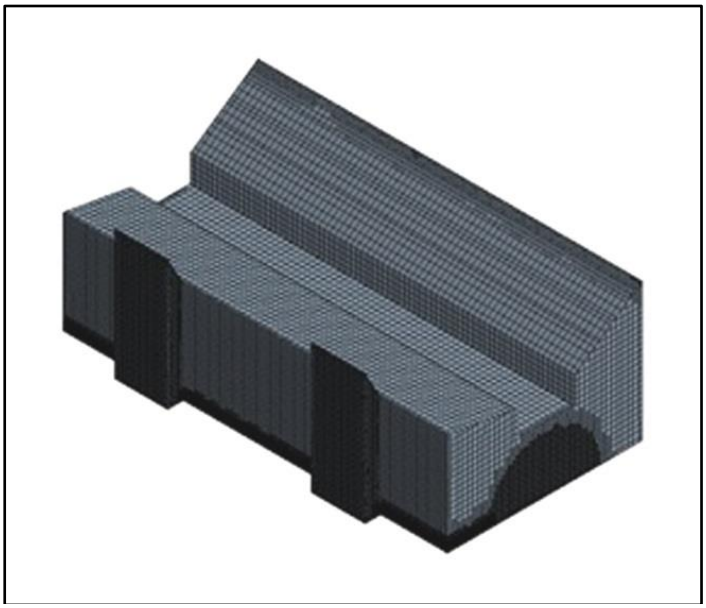

Figure 4: Computational domain of approximately volumes

2.3 Simulation strategy

The simulation strategy used is described in Table 1. The right hand of Table 1 shows the design parameters that were investigated. The left hand shows the results of the volume flow rates for both chimneys. Simulation number 569 was used as a basis for comparison; therefore the results of simulation number 569 appear in the graphs of results (Figures 4-8).

Table 1: Simulation strategy

Summary of Results: Volume Flow Rate (m^3/s)				Design Parameters				
Simulation Number	**Chimney 1**	**Chimney 2**	**Total flow rate**	**Wall Temperature (°C)**	**Floor Grill Width (mm)**	**Chimney Inlet Position**	**Chimney inlet Area (m^2)**	**Chimney Height Above Roof (m)**
567	0.32	0.32	0.63	40	300	bottom	0.6	0
568	0.41	0.41	0.83	55	300	bottom	0.6	0
569	0.49	0.49	0.99	70	300	bottom	0.6	0
570	0.54	0.54	1.09	80	300	bottom	0.6	0
571	0.50	0.50	1.00	70	400	bottom	0.6	0
572	0.50	0.50	0.99	70	500	bottom	0.6	0
573	0.59	0.59	1.18	70	300	bottom	0.6	1
574	0.67	0.67	1.35	70	300	bottom	0.6	2
575	0.35	0.16	0.51	70	300	chimney inlet halfway	0.6	0
576	simulation failed to converge			70	300	chimney inlet at the	0.6	0
577	0.60	0.59	1.19	70	300	bottom	0.9	0
578	0.62	0.62	1.25	70	300	bottom	1.2	0
634	0.52	0.52	1.03	70	3 x 300 grill	bottom	0.6	0
635	0.56	0.56	1.12	40	500	bottom	1.2	2

3 Results and discussion

3.1 Effect of chimney wall temperature on chimney air flow rate

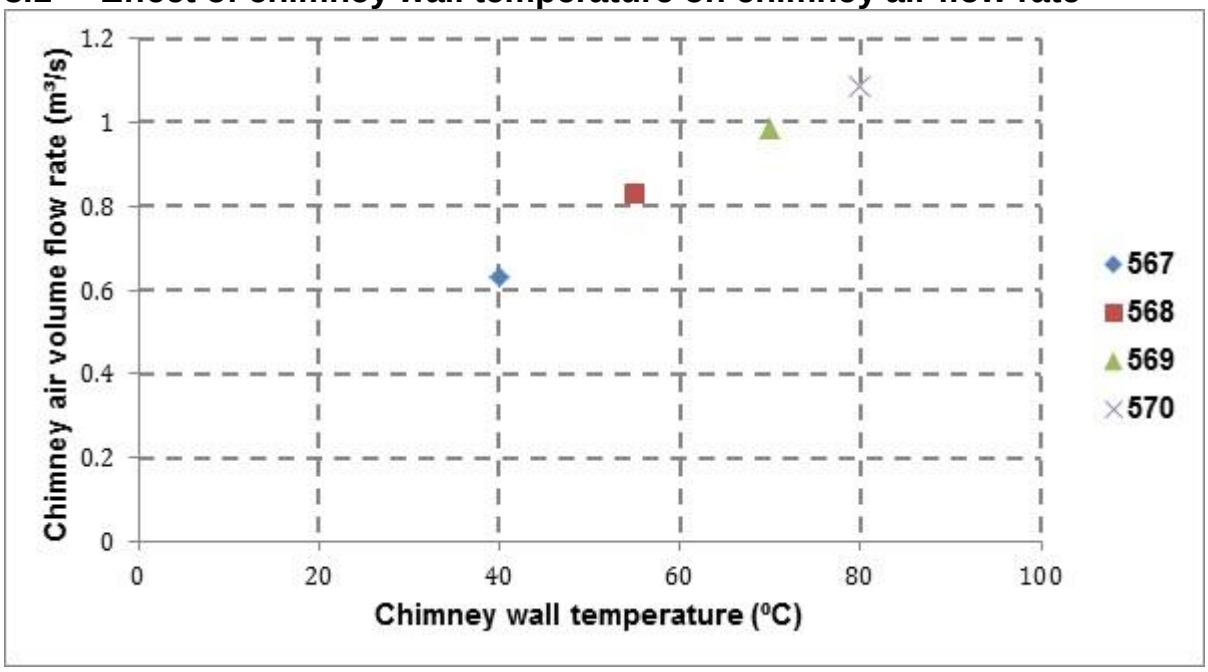

Figure 5: Effect of chimney wall temperature on chimney air flow rate (Refer to Table 1 for related design parameters for given simulation numbers)

Figure 5 shows the inside chimney wall temperature on the horizontal axis and chimney air floor rate on the vertical axis. Figure 4 indicates that there is a linear relationship between the chimney wall temperature and chimney air flow rate. Increasing chimney wall temperature increases chimney air flow rate. Therefore a high chimney wall temperature is desired for a maximum building interior air change rate (See Figure 1, equation 1).

A high chimney wall temperature can be achieved by painting the chimney walls with high solar absorptance paints such as matt black paint. It is highly recommended that the absorbing solar chimney walls be constructed from high thermal mass building materials such as brick and concrete. This ensures a substantial sensible heat storage in the walls which can drive air flow in the chimney for longer periods during overcast periods and prolong the effectiveness after sunset.

3.2 Effect of floor grille width on chimney air flow rate

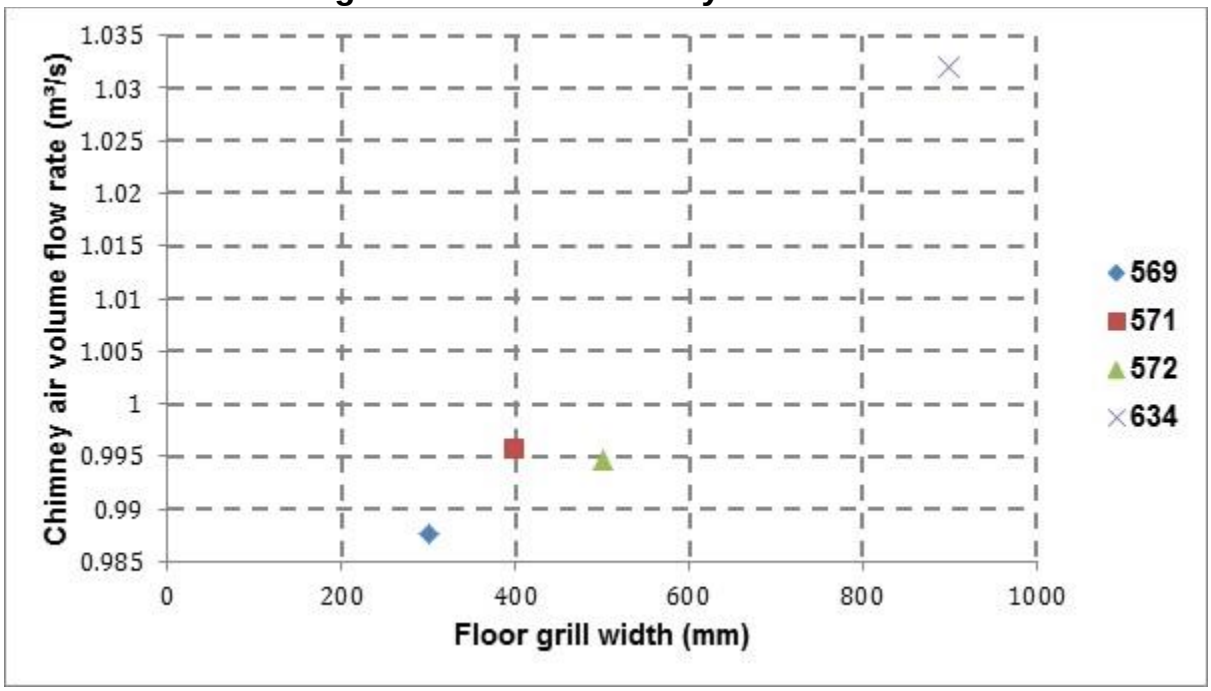

Figure 6: Effect of floor grille width on chimney air flow rate (Refer to Table 1 for related design parameters for given simulation numbers)

Figure 6 illustrates the air inlet floor grille width on the horizontal axis and chimney air floor rate on the vertical axis. Note that simulation 634 in Figure 6 is a combination of three separate air inlet floor grilles with a grille width of 300 mm each, which adds up to a 900 mm air inlet grille width (See Figure 7). Figure 6 indicates that increasing the grille width from 300 mm to 400 mm increases the chimney air flow rate. Figure 6 also indicates, somewhat counterintuitively, that increasing the grille width from 400 mm to 500 mm begins to reduce the chimney air flow rate. These results indicate that there is an optimum air inlet grille width beyond which a poorer solar chimney performance will result. This result can also be interpreted as, beyond 400 mm air inlet grille width, the buoyancy effect of the solar chimney will be cancelled. This means that natural cross ventilation from windows and doors will reduce the performance of the solar chimney (this effect was not evaluated in any of our simulations). If the solar chimney is to provide ventilation on wind still days, the doors and windows should be shut. However if it is a windy day the user can decide to rather use windows to provide natural ventilation, because the solar chimney is not necessary.

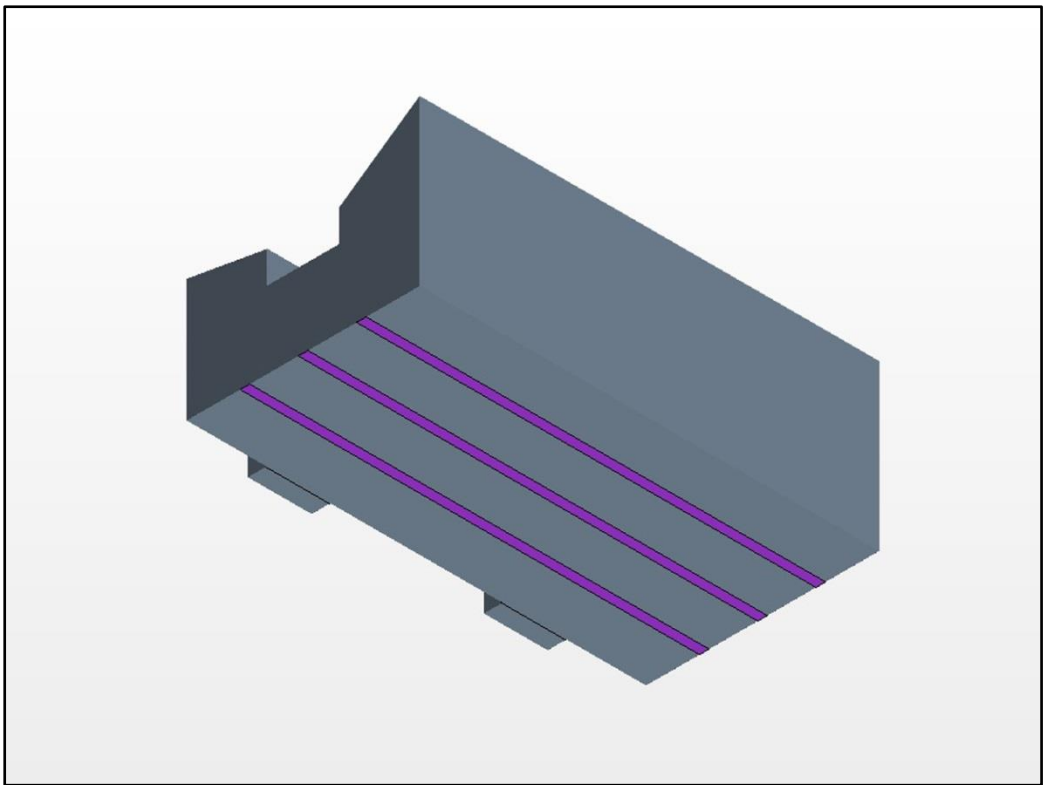

Figure 7: Position of 3 x 300 mm floor grilles coloured in purple

3.3 Effect of chimney height on chimney air flow rate

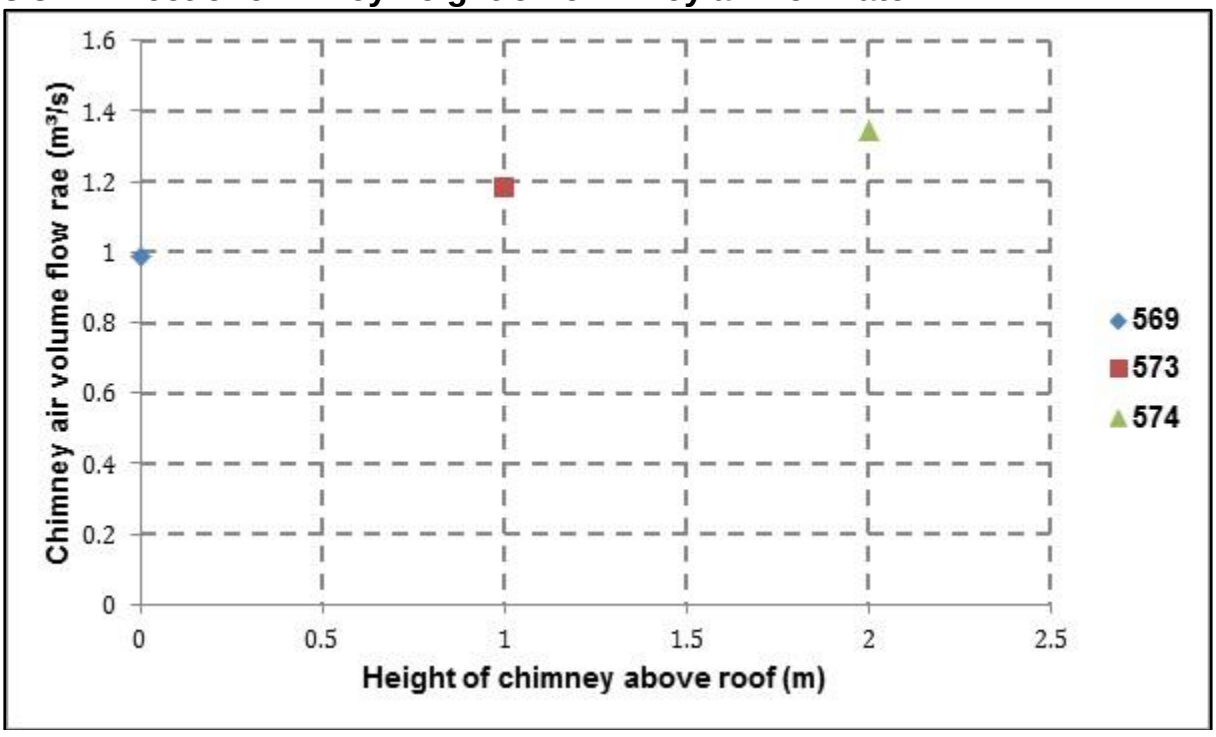

Figure 8: Effect of chimney height on chimney air flow rate (Refer to Table 1 for related design parameters for given simulation numbers)

Figure 8 illustrates the height of the chimney above the roof level on the horizontal axis and chimney air floor rate in the vertical axis. Figure 8 indicates that there is a linear relationship between height of chimney above roof and chimney air flow rate. Increasing height of

chimney above roof increases chimney air flow rate. Although not specifically addressed in this article it is important to note that the chimney should be high enough to ensure that the Neutral Pressure Level (NPL) in the chimney is well above the building to avoid the possibility that hot air enters the building.

3.4 Effect of chimney inlet area on chimney air flow rate

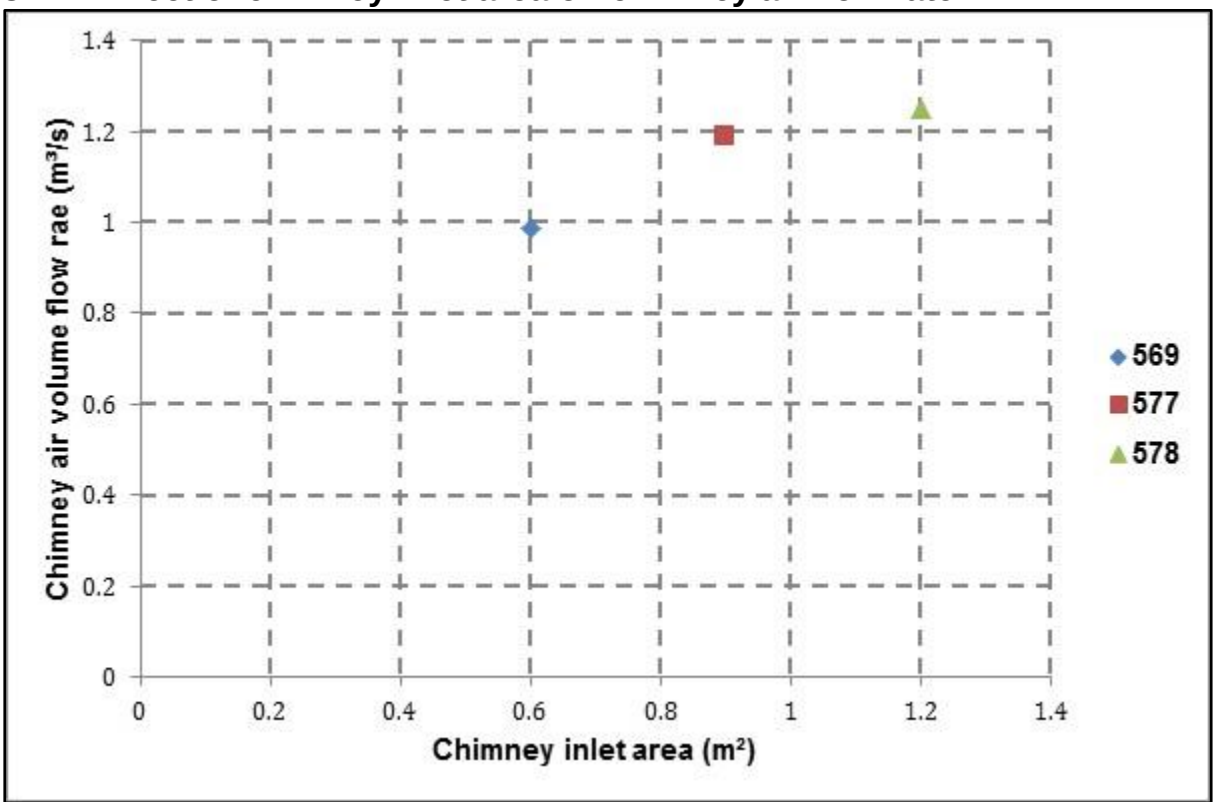

Figure 9: Effect of chimney inlet area on chimney air flow rate (Refer to Table 1 for related design parameters for given simulation numbers)

Figure 9 indicates the chimney inlet area on the horizontal axis and chimney air flow rate on the vertical axis. Figure 9 indicates that there is a big increase of 0.22 m³/s in chimney air flow rate when increasing the chimney inlet area from 0.6 m² to 0.9 m². However a further increase of the chimney inlet area from 0.9 m² to 1.2 m² results in a very small increase of 0.04 m³/ s in the chimney air volume flow rate. Once again this indicates that there is an optimum chimney inlet area beyond which no further improvements in chimney air volume flow rate are realised.

3.5 Results for air flow pattern

The results of Figures 5 to 9 are based on air change rate as an indicator for ventilation performance. However for good ventilation practise, it is not enough to achieve just the prescribed air change rate of fresh outdoor air. An adequate air distribution pattern is also required for replacing all the air of the room, otherwise there may be over-ventilated zones and others where the air is stagnant (Me'ndez *et al*., 2008). Me'ndez, et al., (2008) goes further to describe and explain mean age of air as another ventilation performance indicator. They defined the mean age of air at a point as the mean time that the air particles contained in a differential volume around the point have stayed inside the room. The freshest air (least time in space) will be found at outdoor air inlets, while the oldest air can be found at any other point, not necessarily at the outlets. For instance, if there is a stagnation region or a recirculation region, the mean age of air will be high in these regions and the ventilation will be poor.

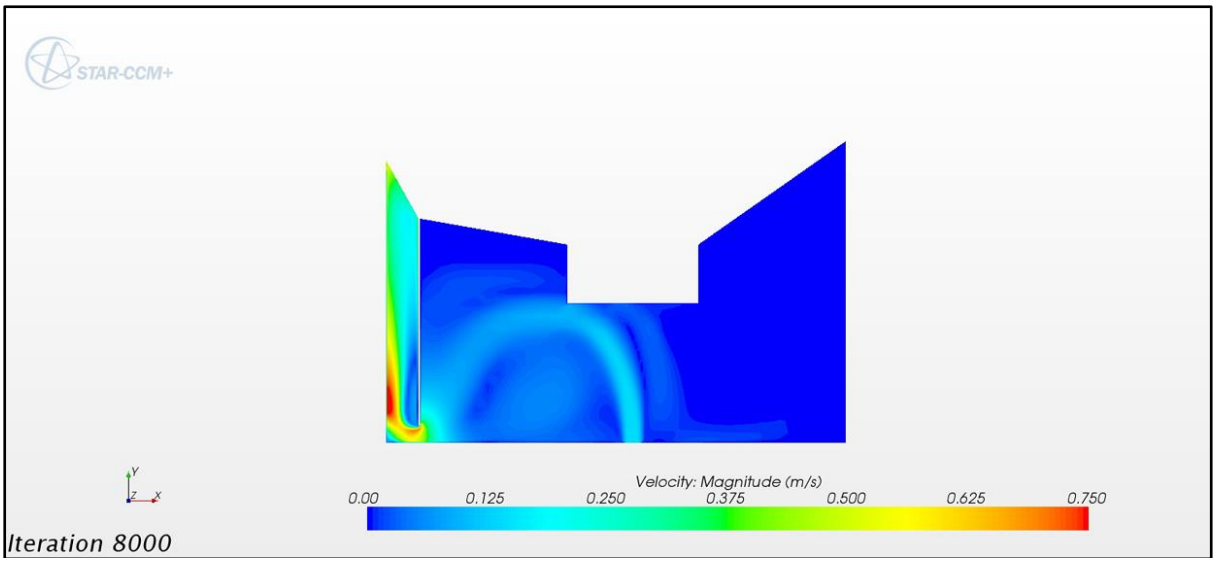

Figure 10: Air velocity distribution within the ventilated space for one floor inlet grill at the middle and chimney inlet located at the bottom

The right side of Figure 10 is entirely blue. This shows that there is little or no air movement on the right side of the building. This means that the mean age of air is high on the right side of building that will lead to poor air quality. This shows that the initial idea of one middle inlet floor grill would cause poor air quality on the right side of the building. A simulation which included three inlet floor grills as illustrated in Figure 7 was done and the air velocity distribution captured in Figure 11 below.

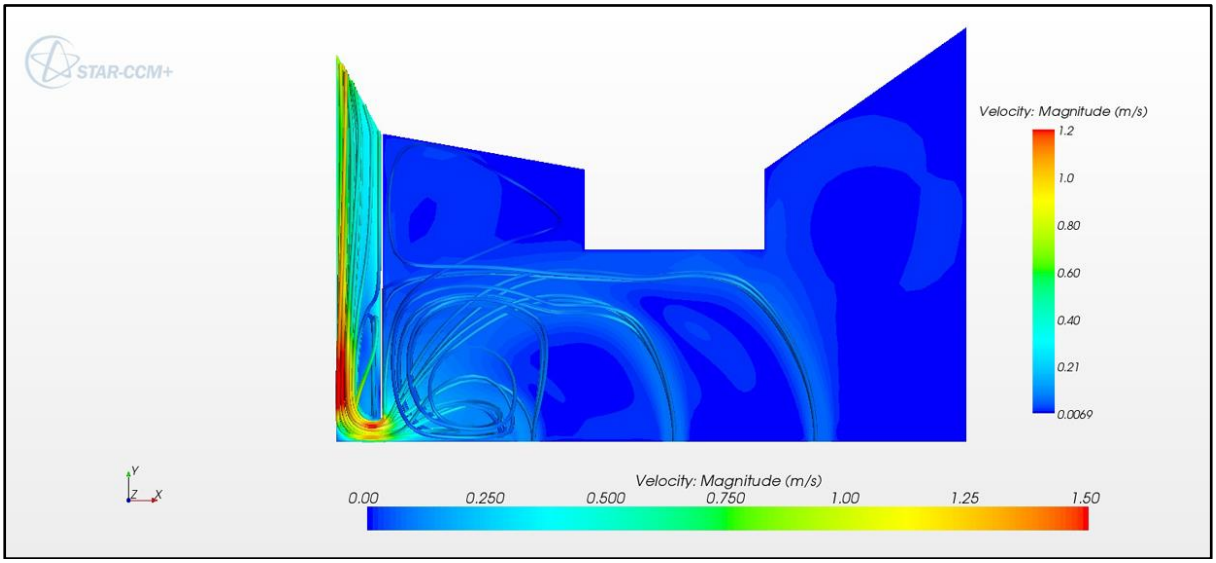

Figure 11: Air velocity distribution within the ventilated space for 3 floor inlet grills and chimney inlet located at the bottom

Figure 11 shows that there is air movement on the left, middle and right sections of the building. Spreading the air inlet floor grills therefore promotes a better distribution of air flow that leads to good indoor air quality.

4 Conclusions

Solar chimneys are not currently widely used in South Africa for a variety of reasons. This chapter quantified the effect of the various design parameters on the efficiency of the air flow.

The study indicated that all the design parameters investigated affect the ventilation performance of the solar chimney.

It was also discovered that there is an optimum beyond which no significant improvement in air flow is realised or even a reduction in efficiency might occur.

The precedent study for the University of Fort Hare teaching complex in East London (Stratford, 2012) and the simulations ran in this study clearly prove that buoyancy driven ventilation systems such as Trombe walls and solar chimneys do work well if they are designed properly. Furthermore they perform well in a hot and sunny country such as South Africa that provides sufficient temperature differentials to drive the chimney. Buoyancy driven ventilation systems continue to function in wind still conditions that are often found in places such as Pretoria. Over and above sufficient air changes per hour the distributed placement of floor inlets will ensure a air distribution and good air quality.

5 References

Cengel, Y.A., 2008. *Introduction to thermodynamics and heat transfer*. 2nd ed. Reno, Nevada, USA: McGraw-Hill.

Chartered Institution of Building Services Engineers (CIBSE), 1997. CIBSE applications manual AM10 natural ventilation in non-domestic buildings. London: CIBSE.

Gontikaki, M., 2010. *Optimisation of a solar chimney to enhance natural ventilation and heat harvesting in a multi-storey office building.* March. Technical University of Eindhoven. Available at: http://www.bwk.tue.nl/bps/hensen/team/past/master/Gontikaki_2010.pdf [Accessed 3.04.2014].

Mendez, C., San Jose J.F., Villafruela, J.M. and Castro, F., 2008. Optimization of a hospital room by means of CFD for more efficient ventilation. *Energy and Buildings*, 40(2008), pp.849–854.

Stratford, A. 2012. University of Fort Hare: new Auditoria and Teaching Complex: East London Campus. In *Green building Handbook*, Volume 4, pp. 157-163.